CHAPTER 116

The Interaction of Waves and Currents over a Longshore Bar

I.A. Svendsen & J. Buhr Hansen *

Abstract

A two-dimensional model for waves and steady currents in the surf zone is developed. It is based on a depth integrated and time averaged version of the equations for the conservation of mass, momentum, and wave energy. A numerical solution is described based on a fourth order Runge-Kutta method. The solution yields the variation of wave height, set-up, and current in the surf zone, taking into account the mass flux in the waves.

In its general form any wave theory can be used for the wave properties. Specific results are given using the description for surf zone waves suggested by Svendsen (1984a), and in this form the model is used for the wave motion with a current on a beach with a longshore bar. Results for wave height and set-up are compared with measurements by Hansen & Svendsen (1986).

1. Introduction

On a beach with a longshore bar the wave breaking over the bar is usually combined with a net shoreward mass flux which, in a three-dimensional flow situation, feeds longshore currents.

Both field observations and experiments indicate that the longshore current is much stronger in the shore-parallel channel or "trough" behind the bar than on the bar itself. Thus for almost shore-normal waves the motion over the bar can be nearly two-dimensional, at least till a point somewhere around or after the bar crest.

The net flow over the bar and in the trough behind was studied theoretically by Bruun (1963) and later by Dalrymple (1978), who was able to determine the largest possible distance between two successive rip currents. A similar analysis was made by Deigaard (1986). These considerations, however, apply to the creation of the rip over an, in principle, uniform and unbroken bar. Once the rip current has established an opening in the bar the position of the rip is locked to this opening, at least over times long enough for the flow pattern to be considered quasi-steady. Thus the question becomes: how much water flows over the bar with the waves, and how does the net flux influence waves, set-up, etc.?

* Institute of Hydrodynamics and Hydraulic Engineering, Technical University of Denmark, DK-2800 Lyngby, Denmark.

In the present paper we approach these problems theoretically by considering the above-mentioned two-dimensional situation of shore-normal incident waves and a shore-normal current with discharge $\overline{Q}$. In an accompanying paper by Hansen & Svendsen (1986) (denoted by I in the following) this situation is modelled experimentally. The net discharge $\overline{Q}$ is added to the waves well offshore of the slope and runs out through the permeable wave absorber which replaces the actual beach. Thus in this experiment the longshore flow in the trough is not represented.

In choosing this arrangement we implicitly assume that in a prototype situation the magnitude of $\overline{Q}$ will be determined by the distance between the rips and by the position of our two-dimensional flow section relative to the position of the rip currents.

The mathematical numerical model developed is based on the depth integrated, time averaged equations of continuity, momentum, and energy as derived by, e.g., Phillips (1977). These equations apply for a very general combination of waves and currents. In the model, the wave properties, such as radiation stress, mass flux, and energy flux are represented by dimensionless coefficients chosen in a way which makes them depend only weakly on water depth, wave height, and wave period.

The general form of the model allows these coefficients to be determined by any chosen wave theory. In the present application, however, the coefficients are developed using the description of breaking waves suggested by Svendsen (1984a). In that paper, and in Svendsen (1984b) and Hansen & Svendsen (1984), wave height, set-up, and undertow were analysed for breaking waves with no net flow. This is now generalized to include the effect of currents following (or opposing) the waves. This also implies including the effect of the undertow in the wave-current interaction, although in the present form of the model it is only done in a depth-averaged sense.

Finally is presented a comparison with the experimental results for wave heights and set-up over a barred profile described in more detail in I. This is combined with a discussion of the inaccuracies in the theoretical approach as revealed by the comparison.

2. The Basic Equations

The type of model in question belongs to the group of models which consider only the depth integrated equations averaged over a wave period. Thus the effect of the waves on the conservation equations is represented by depth integrated, time averaged quantities, such as (in the continuity equation) the mass (or volume) flux created by the waves, the radiation stress, and (in the energy equation) by the energy flux and the mean energy dissipation per unit of time and area of the bottom.

2.1. Conservation of Mass

Following Phillips (1977) (although with a different notation) we use the definitions shown in Fig. 1. An x,z-coordinate system has its origin in the undisturbed water surface SWL, and the instantaneous water surface elevation $\eta(x,t)$ is measured from the local mean water surface MWS so that the temporal mean of η is zero.

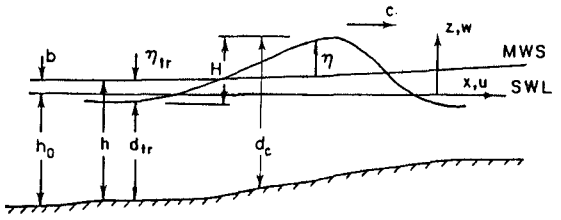

Figure 1. Definitions used.

The horizontal particle velocity u(x,z,t) is divided into two parts u_w (wave) and U (current) defined so that

$$u = u_w(x,z,t) + U(z) \quad ; \quad \overline{u}_w = 0 \tag{2.1}$$

where $\overline{\ }$ means average over a wave period.

We define a depth mean value of U(z) by

$$U = \overline{\frac{1}{h}\int_{-h_0}^{b+\eta} U(z)dz} \tag{2.2}$$

and the volume flux due to the wave part u_w of the motion then becomes

$$Q_s = \overline{\int_{-h_0}^{b+\eta} u_w \, dz} = \overline{\int_{\eta_t}^{b+\eta} u_w \, dz} \quad *) \tag{2.3}$$

where η_t is the (negative) surface elevation in the wave trough. The total mean volume flux $\overline{Q}$ can then be written

$$\overline{Q} = \overline{\int_{-h_0}^{b+\eta} u \, dz} = Q_s + Uh \tag{2.4}$$

Eq. (2.4) is the equation for the conservation of mass.

2.2. Conservation of Momentum

In the present study we will consider only the quasisteady problem of a time-independent current. We also assume that in the depth-integrated and time-averaged momentum and energy equations U(z) can be replaced by U. We can then use the momentum and energy equations given by Phillips (1977).

Following Phillips we define the radiation stress by

*) Notice that this definition of Q_s differs slightly from that by Svendsen (1984b), who used u instead of u_w in (2.3).

$$S'_{xx} = \overline{\int_{-h_0}^{b+\eta} \rho(u_w^2 - w^2)dz} + \frac{1}{2}\rho g\overline{\eta^2} - \frac{\rho Q_s^2}{h} \tag{2.5}$$

where w is the vertical velocity, and ' in S'_{xx} indicates the inclusion of the Q_s-term. This term is actually $O(H^4)$, which is small in ordinary Stokes waves, and it was omitted by Mei (1983). I turns out even in surf zone waves, where H/h = 0.6, to be rather unimportant.

With these definitions and simplifications the horizontal momentum equation can then be written in the following form

$$\frac{d}{dx}\left\{\rho\frac{\overline{Q}^2}{h} + S'_{xx}\right\} + \rho gh\frac{db}{dx} + \overline{\tau}_b = 0 \tag{2.6}$$

which, except for the $\overline{\tau}_b$-term, is the same as Phillips' expression (3.6.11).

2.3. Conservation of Energy

We define the energy flux E_f due to the waves only by

$$E_f = \overline{\int_{-h_0}^{b+\eta} \left\{p_D + \frac{1}{2}\rho(u_w^2 + w^2)\right\} u_w\, dz} \tag{2.7}$$

where p_D is the dynamic pressure defined as

$$p_D = p + \rho g(z - b) \tag{2.8}$$

The energy density E in the waves is

$$E = \overline{\int_{-h_0}^{b+\eta} \frac{1}{2}\rho(u_w^2 + w^2)dz} + \frac{1}{2}\rho g\overline{\eta^2} \tag{2.9}$$

and the total mean dissipation per m^2 bottom and per second is termed $\mathcal{D}$.

The energy equation for the wave motion then becomes

$$\frac{d}{dx}\left\{E_f + UE - \frac{1}{2}\rho\overline{Q}\left(\frac{Q_s}{h}\right)^2\right\} + S'_{xx}\frac{dU}{dx} - \overline{\tau}_b U = \mathcal{D} \tag{2.10}$$

This form also corresponds to Phillips' Eq. (3.6.19) except for the term $\overline{\tau}_b U$, which is the dissipation at the bottom due to the current*). In the surf zone, however, this contribution is very small relative to the total dissipation $\mathcal{D}$, and hence we shall omit it in the numerical computations. $\mathcal{D}$ also includes the dissipation in the bottom boundary layer due to the oscillatory motion, and also that contribution will be ignored in this paper. This implies that $\mathcal{D}$ simply is assumed to equal the breaker disspation.

The two equations (2.6) and (2.10) may be considered generalised versions of the momentum and energy equations often considered in the surf zone

$$\frac{dS_{xx}}{dx} = -\rho gh\frac{db}{dx} - \overline{\tau}_b \quad , \qquad \frac{dE_f}{dx} = \mathcal{D} \tag{2.11}$$

*) See Christoffersen & Jonsson (1980).

Like these two equations, (2.6) and (2.10) can be solved for b and H^2 provided the wave properties are described in terms of h, b, and H^2. Notice, however, that since

$$h = h_0 + b \tag{2.12}$$

even Eqs. (2.11) are complicated.

3. Dimensionless Wave Quantities

As mentioned in the introduction the wave quantities Q_s, S'_{xx}, E_f, and E must all be determined by some wave theory. This also applies to the energy dissipation $\mathcal{D}$ and the mean bottom shear stress $\overline{\tau}_b$. To facilitate a rational approach to this problem we define dimensionless forms of these quantities.

For Q_s, S'_{xx}, E_f, and E we introduce the following dimensionless quantities

$$B_Q = Q_s h/c_r H^2 \tag{3.1}$$

$$P' = S'_{xx}/\rho g H^2 \tag{3.2}$$

$$B = E_f/\rho g c H^2 \tag{3.3}$$

$$B_E = E/\rho g H^2 \tag{3.4}$$

We see that for linear theory these four quantities would depend only on h/L (L being local wave length defined as cT). In nonlinear waves, and particularly breaking waves, the dimensionless quantities will depend also on the wave height, but only weakly so.

The energy dissipation $\mathcal{D}$ is non-dimensionalized by defining D as

$$D = 4\ hT_a/\rho g H^3 \tag{3.5}$$

which is inspired by the idea that the dissipation in breaking waves resembles that in a bore.

The same definitions (except B_Q) were used by Svendsen (1984a), who suggested simple expressions for their form for surf zone waves. Before actually limiting the computations to a particular way of describing the breaking waves we first develop the numerical scheme used for the solution. Thus in the following we simply assume that

$$(B_Q,\ P',\ B,\ B_E,\ D) = f(x) \tag{3.6}$$

where f(x) includes dependence on wave height H, set-up b, and more detailed wave properties such as shape of surface profile, velocity, and pressure distributions, etc. Hence also results for linear theory could be used (although it may not be expected to represent the wave details well).

In the present formulation of the problem we consider $\overline{Q}$ as known (equal to the discharge supplied by the pump). Hence the net current velocity U can be determined from the continuity equation (2.4) as

$$U = \frac{\bar{Q}-Q_s}{h} \tag{3.7}$$

The mean bottom shear stress $\bar{\tau}_b$ will be discussed in Sect. 6.

4. The Numerical Procedure

Christoffersen & Jonsson (1980) showed that for Stokes waves the energy equation for the wave motion corresponding to (2.10) can be written as an equation for conservation of wave action, namely for the steady case considered here as

$$\frac{d}{dx}\left(\frac{E}{\omega_r}(U + c_{gr})\right) + \frac{\mathcal{D} - \bar{\tau}_b U}{\omega_r} = 0 \tag{4.1}$$

where c_{gr} is the Stokes group velocity. This version of the energy equation, however, was derived utilizing the special properties of linear waves and hence cannot be used for the general nonlinear waves considered in this paper. We therefore choose to solve (2.6) and (2.10) directly for b and H^2 respectively.

The numerical solution is obtained by a fourth order Runge-Kutta method. This requires that the two differential equations (2.6) and (2.10) with (3.1) through (3.5) substituted are written on the form

$$\frac{db}{dx} = f_b(x,b,H^2) \quad ; \quad \frac{dH^2}{dx} = f_H(x,b,H^2) \tag{4.2}$$

Since, however, the dimensionless coefficients in general are unknown functions of b and H^2 the form (4.2) cannot be obtained in a strict manner.

We therefore utilize the assumption that the dimensionless coefficient depends only weakly on H. To further simplify the problem we also assume that the additional terms in (2.6) and (2.10) due to the current are small too. For the numerical computations we therefore isolate db/dx and dH^2/dx from the main terms in (2.6) and (2.10), that is the terms included in (2.11). We then accept that derivatives of the dimensionless coefficients, the current, and the Q_s-terms contain db/dx and dH^2/dx. In the computations these db/dx and dH^2/dx are then evaluated only at each grid point, not at intermediate points in each integration interval as the Runge-Kutta method prescribes.

The equations for db/dx and dH^2/dx derived according to these assumptions may be described by introducing the following definitions

$$\alpha = c_r/\sqrt{gh} \tag{4.3}$$

$$D' = D\,\frac{H^2}{h}\,\frac{H}{h}\,\frac{1}{4T_a\alpha\sqrt{g/h}\,B} = \frac{\mathcal{D}}{\rho g c B} \tag{4.4}$$

$$f_1 = \left[\frac{\bar{Q}^2}{gh^3}h_x - \frac{\bar{\tau}_b}{\rho g h}\right] \Big/ \left(1 - \frac{1}{2}P\left(\frac{h}{h}\right)^2\right) \tag{4.5}$$

$$g_1 = \frac{H^2}{E_f}\left[\frac{1}{2}\rho\bar{Q}\,\frac{d}{dx}\left(\frac{Q_s}{h}\right)^2 - S'_{xx}\frac{dU}{dx} - \frac{d}{dx}(EU)\right] \tag{4.6}$$

We then get:

$$\frac{db}{dx} = F_b \tag{4.7}$$

$$\frac{dH^2}{dx} = F_H \tag{4.8}$$

where

$$F_b = -\frac{P'}{h}\frac{D' + H^2\left(\frac{P'_x}{P} - \frac{B_x}{B} - \frac{1}{2}\frac{h_{ox}}{h}\right) + g_1}{1 - \frac{1}{2}P'\left(\frac{H}{h}\right)^2} + f_1 \tag{4.9}$$

$$F_H = D' - \left(\frac{1}{2}\left(\frac{h_{ox}}{h} + \frac{F_b}{h}\right) + \frac{B_x}{B}\right)H^2 + g_1 \tag{4.10}$$

f_1 and g_1 represent the small terms mentioned above. We see that, in addition to contributions that vanish with the net flow $\bar{Q}$, there are terms associated with $\bar{\tau}_b$ or U which for $\bar{Q} = 0$ represents the undertow. Except for the $\bar{\tau}_b$-term all these terms are calculated by differentiating analytically the expressions given in the following Section 5. In the computations we assume that $dB_0/dx = d\alpha/dx = 0$ (see I), and for computation of b_{n+1} and H^2_{n+1} at points x_{n+1}, f_1 and g_1 are evaluated only at x_n.

The fourth order Runge-Kutta scheme for two simultaneous equations is given in, e.g. Hildebrand (1974, 2nd ed.) p. 291.

5. Determination of the Wave Quantities

The mathematical-numerical description presented so far does not presume anything about how the wave properties Q_s, S'_{xx}, E_f, E, and $\mathcal{D}$ are determined. As mentioned a description of the phase motion of the waves must be involved, and most often sinusoidal waves have been used to determine the radiation stress and the energy flux for a wave with a given height and period. Examples are Huang & Wang (1980), Dally et al. (1984), Izumiya & Horikawa (1984). But also solitary waves and cnoidal wave theory have been used.

For the present applications we determine Q_s, S'_{xx}, E_f, and E by using the model for surf zone waves suggested by Svendsen (1984a).

The basic assumption is that the actual horizontal particle velocity in the oscillatory motion shown in Fig. 2a can be approximated by a constant velocity u_0 everywhere except in the surface roller (Fig. 2b). Here the velocity is assumed to be equal to the phase velocity c, since the roller represents a body of water which is carried with the wave. It is furthermore assumed that the pressure is hydrostatic.

Following Svendsen (1984a) we also assume that u_w can be approximated by

$$u_w \simeq c_r \eta/h \tag{5.1}$$

where c_r is the wave speed relative to the water.

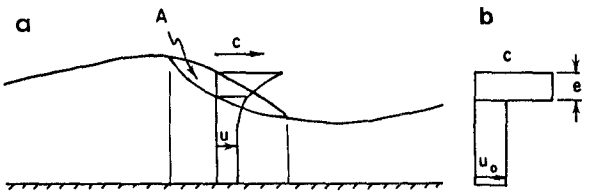

Figure 2. Actual and assumed velocity profiles.

The inaccuracies this leads to are analysed in some detail in I.

c_r, U, and the wave speed c_a observed from a fixed point are related by

$$c_a = c_r + U \tag{5.2}$$

From the definition (2.3) for the volume flux Q_s due to the waves we then get the following for B_Q (defined by (3.1))

$$B_Q = B_0 + B_r \frac{gh}{c_r^2} \tag{5.3}$$

where

$$B_0 \equiv \overline{\left(\frac{\eta}{H}\right)^2} \tag{5.4}$$

$$B_r = \frac{A}{H^2} \frac{c_r}{gT_r} \tag{5.5}$$

Here A is the vertical cross-sectional area of the roller. Svendsen (1984a) found $A/H^2 \sim 0.9$. T_r is the relative wave period which is related to the absolute period T_a through (5.2) by $L \simeq c_r T_r = c_a T_a$. (Notice that owing to the different definition of Q_s, the result for Q_s differs by a factor h/d_t from the result given by Svendsen (1984b). d_t is the water depth under the wave trough, Fig. 1.)

Similarly, we get from the definition (2.5)

$$P' = B_0\left(\frac{1}{2} + \frac{c_r^2}{gh}\right) + B_r - \frac{c_r^2}{gh}\left(\frac{H}{h}\right)^2 B_Q \tag{5.6}$$

(2.7) yields for B

$$B = B_0 + \frac{1}{2} B_r \tag{5.7}$$

and finally, (2.9) yields

$$B_E = \frac{1}{2}\left\{B_0\left(1 + \frac{c_r^2}{gh}\right) + B_r\right\} \tag{5.8}$$

Equations (5.3) - (5.8) together with (3.1) - (3.4) determine Q_s, S'_{xx}, E_f, and E in the momentum and energy equations ((2.6 and (2.10) respectively) for a wave of given height H and phase velocity c_r at depth h.

As in Svendsen (1984a) we will assume that α in (4.3) is constant throughout the surf zone. This is further discussed in I. An alternative - and perhaps more natural - choice would be to assume that c_r equals the speed of a bore with height H. However, in I it is found that the difference is small, and α constant is much simpler to use in the derivations.

Following Svendsen (1984a) we assume that the energy dissipation can be determined as the dissipation in a bore of the same height as the wave. This results in

$$\mathcal{D} = - \rho g \frac{c_r}{L} h \frac{H^3}{4 d_t d_c} \tag{5.9}$$

where d_t and d_c are instantaneous water depths below the wave trough and the wave crest respectively. In establishing this analogy to the bore it is assumed that adding a uniform current to the wave or the bore does not change the breaking process. Therefore, the phase velocity in (5.9) is the relative velocity c_r.

Eq. (5.9) is substituted into the definition (3.5) and we utilize that (5.2) implies

$$T_r = T_a(1 + U/c_c)^{-1} \tag{5.10}$$

This then yields

$$D = - \frac{h^2}{d_t d_c} \frac{1}{1 + U/c_r} \tag{5.11}$$

This expression illustrates that for a current U > 0 following the wave the dissipation decreases relative to a wave of the same absolute period T_a and vice versa for a wave on an opposing current, as one would expect from the corresponding change in wave steepness.

6. The Mean Bottom Shear Stress

The mean bottom shear stress $\overline{\tau}_b$ occurs in the time-averaged momentum equation (2.11). Svendsen et al. (1987) showed how $\overline{\tau}_b$ can be determined from the undertow, which is patched to the flow in the (oscillatory) bottom boundary layer to satisfy the no-slip condition at the bottom. This implies that to determine $\overline{\tau}_b$ we must first determine the velocity distribution over depth of the undertow (which here means the current velocity profile U(z)). Their results for $\overline{\tau}_b$ are equivalent to

$$\overline{\tau}_b = \frac{1}{2} \rho f_w u_{wbm} U_b \tag{6.1}$$

where f_w is the wave friction factor, u_{wbm} is the particle velocity amplitude at the bottom, and U_b the current velocity at the bottom (i.e. outside the boundary layer).

In the present version of the model we will approximate (6.1) by

$$\bar{\tau}_b = \frac{1}{2} \rho f_w u_{wbm} U \tag{6.2}$$

(U given by (2.2)). As the measurements in I show, this is not always a good approximation and may for small U even lead to (small) $\bar{\tau}_b$ values of the wrong sign. The total error on b, however, is estimated not to exceed 20% of this already very small contribution (in numbers less than 0.2·1.2 mm of a total set-up of ~15 mm for the experiments in I).

For u_{wbm} we have used the forward velocity amplitude

$$u_{wbm} = c \frac{\eta_c}{H} \frac{H}{h} \tag{6.3}$$

and f_w is found from Jonssons's diagrams to be $\sim 2 \cdot 10^{-2}$.

7. Comparison with Experimental Results for Waves and Currents Over a Longshore Bar

Numerical experiments have been carried out with the model for the wave-current flow over the longshore barred profile investigated experimentally in I.

In these experiments the still-water depth h_0 is given by (all units in m)

$x < 14.78$ $\qquad h_0 = 0.340$

$14.78 < x < 22.96$ $\qquad h_0 = 0.340 - (x - 14.78) \cdot 0.0280$

$22.96 < x$ $\qquad h_0 = 0.0705 + (x - 25.70)^2 \cdot 5.53 \cdot 10^{-3}$

This corresponds to a plane bottom with slope $h_x = 0.0280 = 1 : 35.7$ between $x = 14.78$ and $x = 22.96$, succeeded by a parabola with summit (bar crest) at $x = 25.70$.

The numerical experiments described here were made with the following (fixed) parameter values (see I):

$A/H^2 = 0.9$; $B_0 = 0.090$

$\eta_c/H = 0.60$; $\alpha = 1.0$

$\Delta x = 0.1$;

Formally, A/H^2 represents the roller, and the value of 0.9 was obtained from deep water measurements (see Svendsen, 1984a).

The choice of B_0 constant and $\alpha = 1$ may be refined on the basis of the experimental results in I. The formulas for the coefficients show that changes in B_0 or α will effect results in much the same way.

The discussion is mainly restricted to the wave height and the set-up variations. Fig. 3 shows a comparison of wave heights for the four $\bar{Q}$-values for which measurements are reported in I, and Fig. 4 shows the set-up. Two sets of computations are shown:

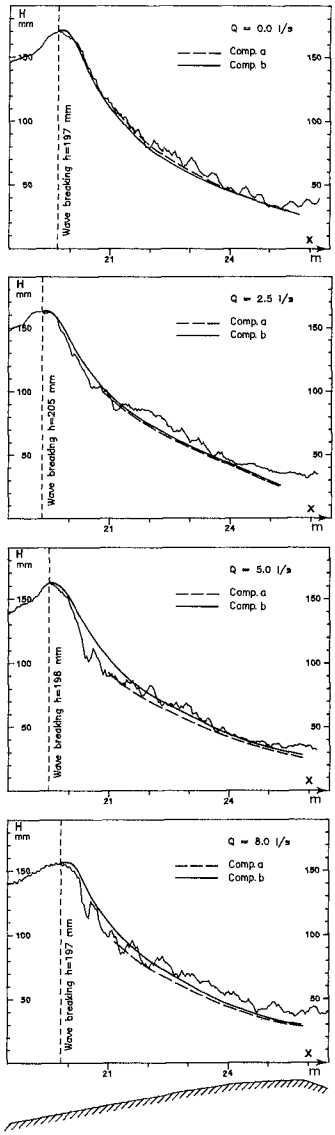

Figure 3. Comparison of measured and computed wave heights.

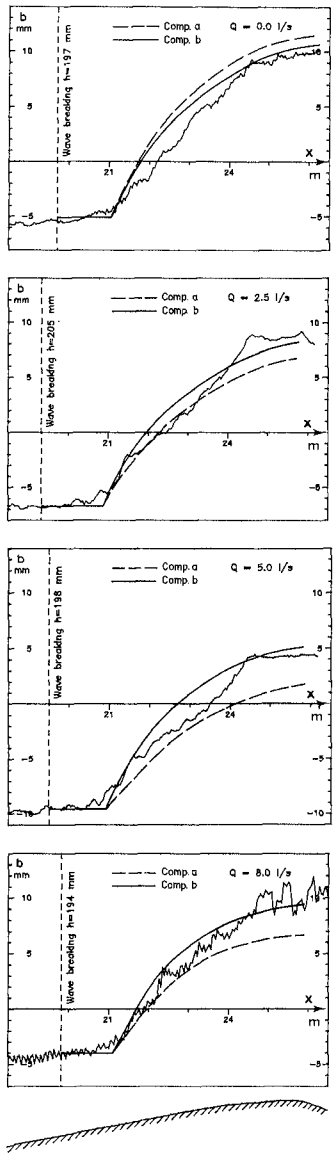

Figure 4. Comparison of measured and computed set-up values.

a) Computations starting at $h_o = 0.8\ h_{oB}$. This point was found by Svendsen (1984a) to correspond to the end of the transition region, in which the collapse of the wave creates an almost constant S_{xx} in spite of the decrease in wave height.

b) Computations starting from the breaking point. In this case the dissipation has artificially been made to grow gradually from 0 at the breaking point and asymptotically approach the value given by (5.9). The expression used is

$$\mathcal{D} := \tanh\left(0.4\ \frac{x - x_B}{h_{oB}}\right)\mathcal{D} \tag{7.1}$$

which implies that at a distance of five times h_{oB} $\mathcal{D}$ has reached 96% of the full value. This modification does not model the simultaneous transitions in S'_{xx} and E_f, and hence (7.1) is combined with the assumption $b_x = 0$ in $x_B < x < x_t$ (x_t representing the transition point). For a more detailed discussion of the transition region reference is made to Basco (1986).

7.1. General Comparison

It is seen from Fig. 3 that the wave height variation is quite accurately predicted by the model with a slight tendency to too low values. It may also be noted that, in spite of the fact that computation a) starts at the transition point with a wave height which is somewhat different from the height obtained by computation scheme b) at that point, the wave heights obtained near the bar crest by the two schemes are nearly the same.

Also the set-up values over the bar crest are in reasonable agreement with the measurements, whereas there is a general tendency to too high b-values in the region between the transition point and the bar crest. In particular, it is noticed that immediately after the transition point the computations have db_x/dx significantly larger than the measurements.

As should be expected, the set-up variation depends strongly on the wave heights. This can be seen by comparing the set-up variations from a) and b) in the four cases and noting that in some cases the wave heights from computation b) are larger than those from a), in some not: the computed set-up variations follow the same pattern. The coupling from set-up to wave height is simply represented by the fact that the set-up represents an increase in depth, which for sufficiently small h_0 may be appreciable.

7.2. The Influence of the Currents

The computations all use measured values of H and b as initial values, and it is seen that in the experiments there are small differences in the mean water level at the breaking point for the four cases. These are caused by small variations in the total amount of water in the flume required to obtain the same mean water depth with the current only.

Computations with the model show that these small differences in the mean water depth do not influence the wave heights and the set-up in the region studied. Therefore, we may get an estimate of the actual effect the current has on the set-up by comparing the set-up variations relative to a common starting point. This is done in Fig. 5, which also shows the wave height variations (see also I, Table 2).

Both wave height and set-up are seen to be almost unaffected by the current.

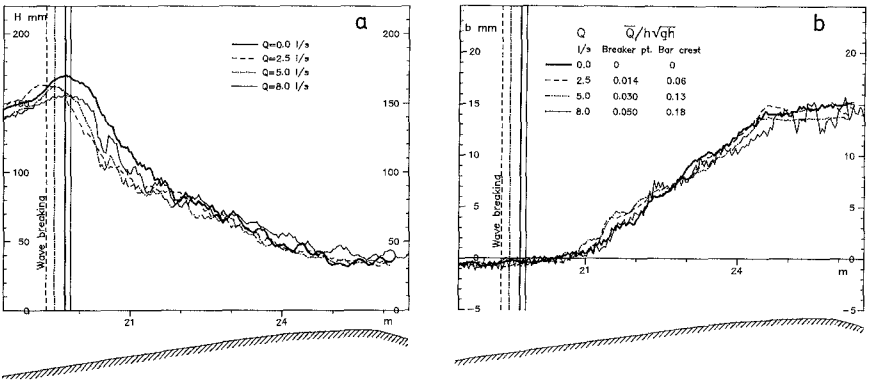

Figure 5. Wave heights (a) and set-up (b) measured for four different values of $\overline{Q}$.

From these results one might jump to the conclusion that the currents have only a negligible effect on the wave conditions. A closer inspection and numerical experiments show that this is too much of a simplification. The extra terms in the equations are important. They just happen nearly to balance each other for the conditions studied.

For the wave heights the behaviour is quite different from a situation with non-breaking waves. The mechanism seems to be that an increase in wave height will also cause an increase in the dissipation and in the energy flux. Hence there is a strong conservatism built into the system at this point, as computations a) and b) also indicated.

For the set-up the mechanism is different: There is no stabilizing effect which parallels that of the dissipation. It is found that the interaction terms in the momentum equation decrease the set-up slightly for all $\overline{Q}$-values, and the bottom shear stress amplifies this by causing a similar decrease in the set-up (up to about 1.2 mm for $\overline{Q} = 8$ ℓ/s). A somewhat stronger effect, however, of the current is caused by the (seemingly) small changes of the wave height described above. That this is the case can be verified in the numerical model by running experiments with the current effect suppressed in one equation and not in the other.

It is particularly interesting to notice that the total set-up Δb at the bar crest measured relative to the water level at the breaking point varies only slightly with the current condition. The measured and computed values are shown in Table 1 below. Considering the many approxima-

tions which the model represents, the very good agreement with the measured values for Δb must be considered fortuitous, as is also suggested by the deviations for the set-up at other x-values.

Notice that the integrated effect of $\overline{\tau}_b$ changes sign when the current increases. This is because shortly after breaking the undertow dominates the (nearbottom) flow ($\overline{\tau}_b < 0$). For large values of $\overline{Q}$ this situation is reversed further shorewards for continuity reasons.

Table 1. Total difference Δb between water level at breaking and over the bar crest.

Discharge $\overline{Q}$ (ℓ/s)	Computation b), $\overline{\tau}_b = 0$	Computation b), $\overline{\tau}_b$ from (6.2)	Measured
0	1.52 cm	1.57 cm	1.55 cm
2.5	1.52 cm	1.51 cm	1.61 cm
5	1.49 cm	1.43 cm	1.42 cm
8	1.39 cm	1.27 cm	1.45 cm

7.3. Inaccuracies in the Predicted Set-Up

The set-up is a direct measure of the variation in shore-normal radiation stress, and the variation of the radiation stress in general is closely associated with the generation of surf zone currents (also in the 3D case). It must therefore be considered an essential condition for a surf zone model that it is able accurately to predict the set-up. At the same time, the set-up is fairly easy to measure and hence a convenient quantity to test models against.

As mentioned earlier Fig. 5 shows that for all $\overline{Q}$-values there is a tendency that the model overestimates the growth rate of the set-up immediately after the transition point (where the momentum equation is switched on in the computations). This inaccuracy was not observed when a model based on the same principles (but without a current) was applied to waves on a plane slope (Svendsen, 1984a). Although the general agreement with measurements might be considered acceptable, and better than other surf zone models, the deviation in db/dx is important. It will cause rather significant discrepancies when db/dx is applied as input for determination of the vertical velocity distribution for the current (see, e.g. Svendsen et al., 1987).

A closer analysis of the situation in the region around the transition point indicates that a major reason for the deviations is related to the abrupt switch between S'_{xx} constant in the transition zone and the rapidly changing S'_{xx} following from the bore description for the inner region. In real waves this transition will of course be gradual.

8. Conclusions

A two-dimensional model for the wave-current interaction in the surf zone has been established. It is based on depth-integrated time-averaged equations of continuity, momentum, and energy. As a description of the

breaking waves is used a generalized form of the method developed by Svendsen (1984a). In principle, however, any wave theory can be used for determination of the coefficients describing the wave properties in the model. The effect of the bottom shear stress is included.

Numerical results for wave heights and set-up are compared with measurements for a bar-type profile. In general, the agreement is found to be quite good although there is a region shortly after the transition point with less accuracy for the set-up.

Finally, the effects of the different elements of the model are discussed.

References

Basco, D.R. (1986), Toward a simple model of the wave breaking transition region in surf zones. Proc. 20th Int. Conf. Coast. Engrg., Taipei.

Bruun, P. (1963), Longshore currents and longshore troughs. J. Geophys. Res. 68, 1065-1078.

Christoffersen, J.B. & I.G. Jonsson (1980), A note on wave action conservation in a dissipative current wave motion. Applied Ocean Res., 2, 4, 179-182.

Dally, W.R., R.G. Dean & R.A. Dalrymple (1984), A model for breaker decay on beaches. Proc. 19th Conf. Coast. Engrg., Houston, 82-98.

Dalrymple, R.A. (1978), Rip currents and their causes. Proc. 16th Int. Conf. Coast. Engrg., Hamburg.

Deigaard, R. (1986), Longshore current behind bars. Inst. Hydrodyn. and Hydr. Engrg., Progr. Rep. 64, 25-29.

Hansen, J.B. & I.A. Svendsen (1984), A theoretical and experimental study of undertow. Proc. 19th Int. Conf. Coast. Engrg., Houston, Ch. 151, 2246-2262.

Hansen, J.B. & I.A. Svendsen (1986) (I) Experimental investigation of the wave and current motion over a longshore bar. Proc. 20th Int. Conf. Coast. Engrg., Taipei.

Hildebrand, F.B. (1974, 2nd ed.), Introduction to numerical analysis. McGraw-Hill, 669 pp.

Izumiya, T. & K. Horikawa (1984), Wave energy equation applicable in and outside the surf zone. Coast. Engrg. Jap., 27, 119-137.

Mei, C.C. (1983), The applied dynamics of ocean surface waves. John Wiley & Sons, 740 pp.

Phillips, O.M. (1977), The dynamics of the upper ocean. Cambridge Univ. Press (2nd ed.), 336 pp.

Stive, M.J.F. & H.G. Wind (1982), A study of radiation stress and set-up in the nearshore region. Coastal Engrg. 6, 1-25.

Svendsen, I.A. (1984a), Wave heights and set-up in a surf zone. Coastal Engrg. 8, 303-329.

Svendsen, I.A. (1984b), Mass flux and undertow in a surf zone. Coastal Engrg. 8, 4, 347-365.

Svendsen, I.A. & P. Justesen (1984), Forces on slender cylinders from very high waves and spilling breakers. Symp. on Description and Modelling of Directional Seas, Techn. Univ., Denmark, June 1984.

Svendsen, I.A., H.A. Schäffer & J. Buhr Hansen (1987), The interaction between the undertow and the boundary layer flow on a beach. Subm. for publ.

Wang, H. & W.-C. Yang (1980), A similarity model in the surf zone. Proc. 17th Int. Conf. Coast. Engrg., I, Ch. 33, 529-546.